# Serum miR-29 is increased in mice with early liver fibrosis

KANA MATSUMOTO[1], YUHEI OHSUGI[2], CHISA TAYAMA[2], MOMONE HAYASHI[2], YUMIKO KATO[2], MIZUHO OHASHI[2] and MITSURU CHIBA[1,3]

[1]Department of Bioscience and Laboratory Medicine, Graduate School of Health Sciences, Hirosaki University, Hirosaki, Aomori 036-8564, Japan; [2]Department of Medical Technology, School of Health Sciences, Hirosaki University, Hirosaki, Aomori 036-8564, Japan; [3]Research Center for Biomedical Sciences, Hirosaki University, Hirosaki, Aomori 036-8564, Japan

Received November 17, 2023; Accepted April 17, 2024

DOI: 10.3892/etm.2024.12573

**Abstract.** Non-alcoholic steatohepatitis (NASH) is a fatty liver disease that is not caused by alcohol consumption and is characterized by fatty degeneration, inflammation and hepatocellular damage. Therefore, predicting future fibrosis is critical in the early stages of NASH to prevent disease progression. The present study examined histological changes in the liver as well as microRNA (miR/miRNA) expression changes in the liver and serum of NASH mice model to identify potential biomarker candidates that could predict early fibrosis. This study used 6-week-old C57BL/6NJcl male mice and fed the control with a standard solid diet (CE-2) for breeding and propagation and NASH groups with a high-fat diet [choline-deficient high-fat and 0.1% (w/v) methionine supplemented diet], respectively. Agilent Technologies miRNA microarray was used to investigate microRNA expression in the liver and serum. Hematoxylin and eosin staining of the livers of the NASH group mice during the second week of feeding revealed fatty degeneration, balloon-like degeneration and inflammatory cell infiltration, confirming that the mice were in a state of NASH. The livers of the NASH group mice at 6 weeks of feeding showed fibrosis. Microarray analysis revealed that miRNAs were upregulated and 47 miRNAs were downregulated in the liver of the NASH group. Pathway analysis using OmicsNet predicted miR-29 to target collagen genes. Furthermore, miR-29 was downregulated in the livers of NASH-induced mice but upregulated in serum. These findings suggested that lower miR-29 expression in NASH-induced liver would increase collagen expression and fibrosis. Early liver fibrosis suggests that miR-29 leaks from the liver into the bloodstream, and elevated serum miR-29 levels may be a predictive biomarker for early liver fibrosis.

*Correspondence to:* Dr Mitsuru Chiba, Department of Bioscience and Laboratory Medicine, Graduate School of Health Sciences, Hirosaki University, 66-1 Hon-cho, Hirosaki, Aomori 036-8564, Japan
E-mail: mchiba32@hirosaki-u.ac.jp

*Key words:* microRNA, gene expression, microarray, serum, microRNA-29, fibrosis

## Introduction

Nonalcoholic fatty liver disease (NAFLD) is a condition in which the liver of individuals with little or no history of alcohol consumption has excessive fatty deposits (1). In 2023, NAFLD affects approximately 30% of the adult population worldwide, making it a common chronic liver disease (2). Nonalcoholic steatohepatitis (NASH) is a type of NAFLD characterized by fatty liver degeneration, inflammatory cell infiltration, and balloon-like cell degeneration; persistent inflammation can lead to liver fibrosis (3-4). The risk of cirrhosis and hepatocellular carcinoma rises as fibrosis progresses, and the liver fibrosis stage of NASH is an important prognostic factor (3-5).

A liver biopsy is frequently used to confirm NASH diagnosis and determine the stage of liver fibrosis (6,7). A liver biopsy is required to distinguish NASH, but the number of patients with suspected NASH is growing, and performing the procedure on all patients is difficult (5). Furthermore, liver biopsy is an effected tool for diagnosing NASH. Additionally, the tissue sampled by liver biopsy does not reflect the condition of the entire liver, and variability in histologic characteristics between samples is a challenge (8). Furthermore, there is interobserver variability when evaluating sampled tissue (9). Hence, there is an increased demand for noninvasive alternatives to invasive liver biopsy (10).

Biomarker testing using blood samples is known to be less invasive. Major biomarkers include the liver enzymes aspartate aminotransferase (AST) and alanine aminotransferase (ALT). These are known as common liver injury markers; specifically, ALT has been used to estimate the degree of fibrosis progression in NASH (11). However, ALT is not a NASH-specific biomarker because it also fluctuates in various diseases other than NASH (12). Furthermore, scoring systems, such as the AST to platelet ratio index, Fib-4 index, and NAFLD fibrosis score, which assess fibrosis by combining multiple measures, are useful in determining the severity of fibrosis in NASH but have not been used for its definitive diagnosis (13-15). Furthermore, the cytokeratin 18 fragment (CK18), which has recently gained attention as a NASH biomarker, has been shown to help distinguish between simple fatty liver (NAFL) and NASH in patients with NAFLD (16-17). However, CK18 has not been used for definitive diagnosis, and issues among reagent kits of variability and low sensitivity have been reported (17,18). Therefore, developing a new noninvasive test

for definitive NASH diagnosis and early liver fibrosis detection in NASH is desirable.

MicroRNAs (miRNAs) are short single-stranded RNAs with 21-23 nucleotides. MiRNAs bind to the 3'-UTR region of target mRNAs, inhibit mRNA translation into proteins, and regulate gene expression (19). Recently, miRNAs have been released from cells and are involved in intercellular communication (20). Furthermore, miRNAs are known to change expression in various diseases, and their potential as biomarkers is promising (20,21). This study focused on miRNAs to find biomarkers that can detect NASH-induced liver fibrosis caused early on.

## Materials and methods

*Mice*. We purchased a total of 75 male 5-week-old C57BL/6NJcl mice (body weight, 20.6±0.7 g) from CLEA Japan. All mice were housed in a conventional animal room with 12/12-h light/dark cycle. Treatment began after a 1-week acclimatization period. Mice were observed 2-3 times per day for monitoring, and health or behavior abnormalities were not observed during the rearing period. The NASH model group was fed a choline-deficient high-fat (CDAHFD) supplemented with 0.1% (w/v) methionine (Research Diets Inc., A06071302). The control group was given a commercial standard diet called CE-2 (CLEA Japan). It was not suitable for the purpose of this study, where we wanted to confirm even the appearance of fibrosis, because fibrosis does not appear with a simple high-fat diet, even after long-term feeding. In addition, the methionine/choline-deficient diet is not suitable for long-term rearing because of the significant weight loss of the mice and increased risk of mortality. Therefore, this diet was used in this study to create a NASH model mouse, which has less weight loss and is suitable for long-term observation.

Both groups were fed and watered *ad libitum*, with replacements once a week. All mice were kept under the conditions described above for 1-12 weeks after feeding, with five mice assigned to each week. The sample size was determined to provide adequate statistical treatment. Sampling was done up to 12 weeks after feeding to check the progression of fibrosis. Blood samples from five mice were collected using cardiac blood sampling under anesthesia with the inhalation anesthetic solution isoflurane (Pfizer) at the end of the 0-, 1-, 2-, 4-, 6-, 8-, 10-, and 12-week after feeding. Sampling for the control and NASH groups was conducted on the same day. Anesthesia was administered via inhalation from a small animal anesthesia machine (Muromachi Kikai) that was vaporized to a concentration of 4-5% and maintained at 2-3%. The cervical dislocation was used for euthanasia, and death was determined by the cessation of respiration and heartbeat.

Under anesthesia, 0.5-1.0 ml of blood was received from the heart, and all mice were promptly cervically dislocated to minimize distress. For this study, the criteria for applying the humane endpoint were symptoms of anguish (e.g., self-injury, abnormal posture, breathing problems, squealing), long-term abnormal appearance (e.g., diarrhea, bleeding, vulvar smears), and rapid weight loss (>20% in a few days). No mice during this study required a humane endpoint prior to study termination. The start of anesthesia to the end of blood collection took <10 min per animal. Death was confirmed by respiratory and cardiac arrest. Blood samples were serum-separated immediately after collection. Blood samples were then placed in a Microtainer (Becton Dickinson), and the coagulated blood was centrifuged at 6,000 G for 3 min to separate the serum. Livers were removed from euthanized mice. The experiments with mice were performed twice during the study period and we have confirmed that the data in this study are reproducible. The Hirosaki University Ethics Committee for Animal Experiments approved this experiment, which followed the Hirosaki University Guidelines for Animal Experiments (Approval No. AE01-2023-004).

*Tissue fixation and tissue block preparation*. Liver tissues that had been excited after perfusion fixation were fixed with 4% (w/v) paraformaldehyde for 48 h and paraffin-embedded blocks were prepared using a Sakura-sealed automatic fixation and embedding device (Sakura Finetek Japan) and Tissue-Tek TEC5 (Sakura Finetek Japan).

*Hematoxylin and eosin (HE) staining*. Paraffin-embedded tissue blocks were thinly sliced to a 4-$\mu$m thickness and attached to glass slides. We deparaffinized tissue sections with xylene and ethanol then rinsed them with water for 5 min. Nuclear staining was conducted in Meyer's hematoxylin solution (Fujifilm Wako) for 1 min, followed by color removal in warm water for 10 min. The samples were then stained with 0.5% (w/v) eosin Y in 80% (v/v) ethanol solution (Fujifilm wako) for 10 sec, rinsed with water to remove the excess staining solution, and fractionated with 75% (v/v) ethanol. The samples were treated with ethanol and xylene before being sealed with Marinol (Muto Chemical) and cover glass (Matsunami Glass).

*Sirius red staining*. Glass slides with paraffin-embedded sections attached were rinsed with running water for 5 min following deparaffinization and hydrophilic treatment. Sirius red staining solution was created by combining 100 ml of saturated picric acid solution with 3 ml of 1% (w/v) Sirius red solution (Fujifilm Wako). The glass slides were rinsed under running water for 5 min after being stained with Sirius red staining solution for 10 min to remove the color. The slides were then dehydrated using ethanol, permeated with xylene, and sealed with Marinol (Muto Chemical) and cover glass (Matsunami Glass).

*Immunohistochemical staining*. Glass slides with paraffin sections attached were rinsed with water for 5 min following deparaffinization and hydrophilic treatment. Glass slides were treated with 3% (v/v) $H_2O_2$ for 5 min before being rinsed in water for 5 min to deactivate endogenous peroxidase. Incubation was made in citrate buffer (pH of 6.0) at 115˚C for 5 min to activate antigen. Glass slides were then washed with Tris-buffered saline (TBS) buffer (25 mM of Tris-HCl and 150 mM of NaCl, pH of 7.2) for 5 min before incubating with a drop of blocking solution [5% (v/v) sheep serum in TBS buffer] on glass slides for 30 min at room temperature. Anti-α-smooth muscle actin (α-SMA) rabbit monoclonal antibody (Cell Signaling Technologies, cat. 19245S) was diluted 500-fold in blocking solution, applied to glass slides, and incubated at room temperature for 60 min. The liquid on the glass slides was removed, washed 3 times with TBS

buffer for 5 min, and then incubated dropwise with EnVision + System-HRP-labeled polymer anti-rabbit (Dako, cat. K4003) for 60 min at room temperature. The liquid on the glass slides was removed, washed three times with TBS buffer for 5 min, and colored with 3,3'-diaminobenzidine tetrahydrochloride solution (Sigma-Aldrich). Glass slides were washed with water, nuclear stained with Meyer's hematoxylin solution (Muto Chemical) for 1 min, and the color was removed by washing with warm water for 10 min. They were dehydrated with ethanol, permeated with xylene, and sealed with Marinol (Muto Chemical) and covered glass.

*Pathological evaluation*. A scoring system has been used to assess the histology of NAFLD/NASH in humans (22). Matsumoto *et al* (23) reported a histological evaluation of NAFLD/NASH in mice fed the same CDAHFD diet as us, similar to the human scoring system. In this study, we also used the histological examination of the liver described by Matsumoto *et al* (23).

*Biochemical tests*. Serum AST and ALT were determined by pocH-100iV Diff (Sysmex) at the Hirosaki University Laboratory Animal Facility.

*RNA extraction*. Total RNA was extracted from livers and 200 $\mu$l of serum using ISOGEN II (Nippon Gene) as per the manufacturer's instructions. The total RNA concentration in livers was measured using a NanoDrop spectrophotometer (NanoDrop Technologies). All total RNA from livers had 260/280 nm absorbance ratios ranging from 1.8-2.0. Ethachinmate (Nippon Gene) was used to precipitate total RNA from serum. A Quant-iT RiboGreen RNA Reagent and Kit (Thermo Fisher Scientific, Inc.) was used to determine the total RNA concentration from serum.

*miRNA microarray analysis*. The miRNA Complete Labeling and Hyb kit was used to label miRNAs in 2.5 ng of serum total RNA and 100 ng of liver total RNA. The microRNA Spike In Kit (cat. no. 5190-1934; Agilent Technologies, Inc.) was used to conduct quality checks on the microarray experiments. The RNA samples were labeled with Cyanine 3 (Cy3) fluorescent dye per the manufacturer's instructions. The Cy3-labeled miRNA was incubated for hybridization with miRNA microarray slides (SurePrint G3 Mouse 8x60-K miRNA microarray slides (cat. no. G4872A; Agilent Technologies, Inc.) at 55˚C and 20 rpm for 20 h. Cy3 fluorescence signals on glass slides were detected using a SureScan microarray scanner (cat. no. G4900DA; Agilent Technologies, Inc.), and fluorescence quantification was done with Agilent Feature Extraction 12.0 (Agilent Technologies, Inc.). As a method of evaluating Spike-In, Agilent Feature Extraction 12.0 was used to ensure that the calculated values of LabelingSpike-InSignal and HybSpike-InSignal were both >2.5. A 90% shift normalization was conducted using the obtained data, and GeneSpring GX14.5 software was used for expression analysis. These data were registered with the Gene Expression Omnibus (https://www.ncbi.nlm.nih.gov/geo/query/acc.cgi?acc=GSE252035).

*Prediction of miRNA target genes*. OmicsNet (https://www.omicsnet.ca/) was used to predict the target genes and functions of miRNAs whose gene expression in the liver is affected by NASH.

*Statistical analysis*. The Shapiro-Wilk test confirmed that each population exhibited a normal distribution. An F test was also performed to confirm the variance of the two groups, and all data were confirmed to be equal variance. Values were expressed as mean ±2 standard deviation. Each sample size was determined to be sufficient at n=5 because the standard deviation was sufficiently small. Significant differences in liver weight, AST, and ALT levels between the control and NASH groups were determined using Student's t-test. P-values of <0.05 indicate significant differences and are marked with an asterisk in each graph.

## Results

*Changes in biochemical components and liver tissue structure in NASH mice*. We showed the changes in body weight of mice fed the Control or CDAHDF diet (Fig. SI). Serum AST and ALT levels, which are markers of liver injury, of the control and NASH groups were measured from 0 to 12 weeks after starting a high-fat diet (Fig. 1A, B). Both AST and ALT levels in the NASH group were significantly higher than those in the control group after 1 week of feeding a high-fat diet. Liver weights were then measured from 0 to 12 weeks after the beginning of the high-fat diet (Fig. 1C). The NASH group had a higher liver weight over time, with significant increases at 4 weeks and 8-12 weeks of feeding compared to the control group.

*Histological changes in the livers of NASH-induced mice*. HE, Sirius red, and α-SMA immunohistochemical staining were used to confirm histopathological changes in the liver of NASH-induced mice (Fig. 2). The stained images in the control group consistently showed normal liver histology up to 12 weeks of feeding, regardless of staining method. HE staining revealed fatty degeneration, balloon-like degeneration, and inflammatory cell infiltration throughout the liver at 2 weeks of feeding in the NASH group, with similar findings at 6 weeks. Sirius red staining revealed clear fibrosis at 6 weeks. Further, α-SMA immunohistochemical staining revealed numerous positive cells at 6 weeks of feeding. The observation was continued for 12 weeks, but there were no significant changes compared to the tissue at 6 weeks.

The above staining results were used to calculate scores for hepatic steatosis, inflammation, ballooning-like degeneration, and hepatic fibrosis (Table I). At 1 week of feeding, the score was evaluated as follows: Steatosis grade 2, Inflammation grade 1, Ballooning grade 0, and Fibrosis grade 0. At 2 weeks of feeding, the animals were classified as having Steatosis grade 3, Inflammation grade 2, Ballooning grade 2, and Fibrosis grade 0. Six weeks of feeding were assessed as Steatosis grade 3, Inflammation grade 3, Ballooning grade 3, and Fibrosis grade 2. These pathological analyses suggest that mouse livers at 2-6 weeks of CDAHDF feeding are in the early stages of fibrosis due to NASH.

*Changes in miRNA expression in the liver of NASH mice model*. To investigate the changes in miRNA expression caused

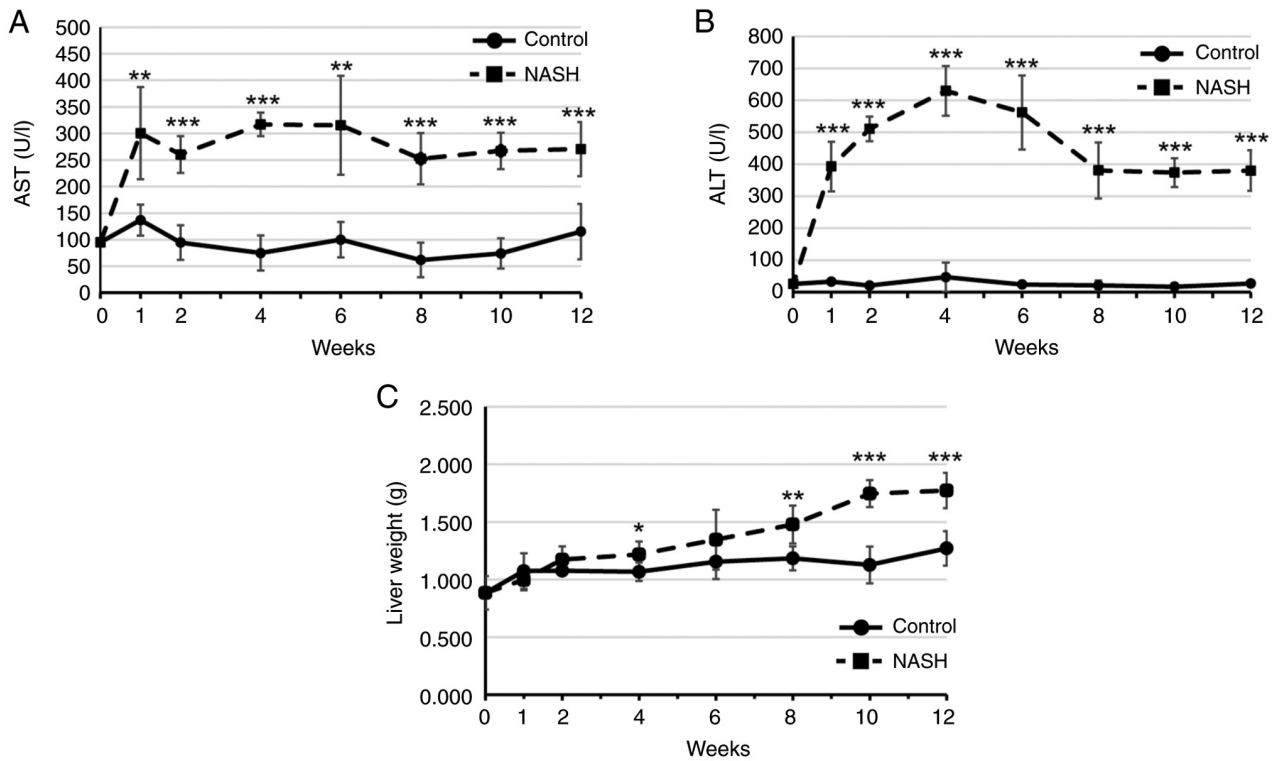


Figure 1. Changes in serum markers of liver injury and liver tissue structure in NASH-induced mice. (A) AST levels in serum. (B) ALT levels in serum. Mice in the control and NASH groups had their AST and ALT levels measured as liver injury markers from 0 to 12 weeks after beginning a high-fat diet feeding with pocH-100iV Diff (Sysmex) according to the manufacturer's instructions. (C) Liver weight changes between the control and NASH groups. Values are presented as mean ±2 standard deviation (SD) (each n=5). $^{*}$P<0.05, $^{**}$P<0.01 and $^{***}$P<0.001 compared with the control. AST, Aspartate aminotransferase; Aspartate aminotransferase, Alanine aminotransferase.

by NASH development, miRNA microarray analysis was performed on livers from the NASH mice model. We investigated miRNA expression in the liver of NASH model mice at 2 weeks of feeding, a NASH state in which fibrosis is not readily visible, based on stained images of liver tissue. Table II lists the miRNAs with an expression difference of more than 1.5-fold compared to the control group. Nine miRNAs were upregulated, while 47 miRNAs were downregulated.

The 47 miRNAs predicted to be downregulated by miRNA microarray analysis in the liver of the NASH group were analyzed using OmicsNet. The target genes of these miRNAs and their associated functions were linked by lines. In the enlarged figure, green circles indicated miRNAs, red circles indicated target genes, and blue circles indicated target genes involved in fibrosis. The relationship between miRNAs and target genes associated with fibrosis predicted a link between the miR-29-3p family and collagen genes in the 47 miRNAs (Fig. 3). A search of the OmicsNet Reactome database for fibrosis-related functions revealed 'collagen formation' and 'collagen biosynthesis and modifying enzymes' (Table SI). Collagen genes play roles in both of these functions, and the miR-29 family was identified as miRNAs that regulate collagen genes.

*Changes in miRNA expression in the serum of NASH mice model*. We performed miRNA microarray analysis in the serum of the NASH mice model at 2 weeks of feeding. Table III shows the miRNAs that had a more than 1.5-fold difference in expression between the NASH and control groups. Twenty-one miRNAs were upregulated, while seven were downregulated. Among the miR-29 family, miR29a-3p and miR-29c-3p, which were linked to collagen genes by OmicsNet results, were upregulated in NASH model mouse serum.

## Discussion

The current study discovered that microarray analysis in a NASH mice model at an early fibrosis the appeared found a link between NASH-induced liver fibrosis and miR-29 (miR-29a-3p and miR-29c-3p). Expression of these miRNAs was reduced in the livers of NASH mice fed a high-fat diet for 2 weeks but increased in serum, suggesting that these miRNAs were released into the blood from the NASH-induced livers.

MiR-29 contains miR-29a, miR-29b, and miR-29c, all of which have different sequences. MiR-29a and miR-29c are encoded on distinct chromosomes in humans and mice, respectively. MiR-29 regulates gene expression, specifically cellular gene expression profiles and protein synthesis. The miR-29 family is important in a variety of biological processes and has been studied concerning diseases and cancers. Previous research has shown that the miR-29 family regulates gene expression in fibrosis (24), neurodegenerative diseases (25), and breast cancer (26). In particular, the miR-29 family has recently received attention for its crucial role in the process of multiorgan fibrosis (24). MiR-29 binds to the 3'-UTR of collagen genes, inhibiting collagen protein expression. Wang *et al* (27) found that reduced miR-29 expression by TGF-β/SMAD signaling in

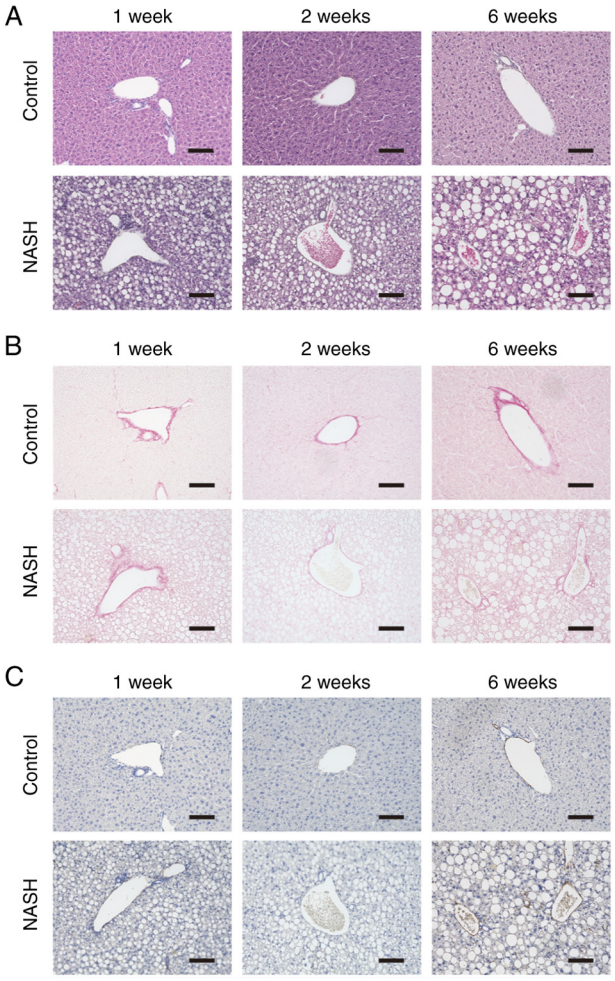


Figure 2. Histological changes in control and NASH groups at 1, 2 and 6 weeks after starting a high-fat diet. (A) Hematoxylin and eosin staining. The NASH group showed numerous small vacuoles in the liver parenchyma, fatty degeneration, hepatocyte ballooning and inflammatory cell infiltration 2 weeks after feeding a high-fat diet. (B) Sirius red staining. Microfibrosis was observed in the liver at 6 weeks after feeding a high-fat diet in the NASH group. (C) α-SMA immunostaining. Positive cells were detected 6 weeks after feeding a high-fat diet in the NASH group. Scale bars, 100 $\mu$m. NASH, Non-alcoholic steatohepatitis.

vascular smooth muscle cells promotes collagen synthesis. Ezhilarasan *et al* (28) recently discovered that miR-29 plays a crucial role in liver fibrosis by regulating collagen gene expression in astrocytes in the liver. Matsumoto *et al* (29) discovered that miR-29a suppressed human liver astrocyte activation and reduced liver fibrosis. Interestingly, Lin *et al* (30) found that miR-29 overexpression suppresses collagen genes, reducing liver fibrosis and inhibiting hepatocyte lipogenesis by lowing PPARγ levels. This suggests that miR-29 not only suppresses liver fibrosis via collagen regulation but also controls NAFLD development. Our miRNA microarray results confirmed a reduction in miR-29 in NASH livers (Table II). Analysis in conjunction with immunohistological analysis of the liver showed a decrease in miR-29 expression in the liver after 2 weeks of consuming a high-fat diet, a stage before α-SMA positivity.

This study found that serum miRNA microarray analysis of mice fed a high-fat diet showed increased serum miR-29a-3p and miR-29c-3p expression after 2 weeks of NASH induction (Table III). Several studies have identified miR-29 as one of the microRNAs that are upregulated in serum in NASH/NAFLD and liver fibrosis (31-34). Our findings support that point. Conversely, Jampoka *et al* (35) found that miR-29a levels were lower in patient serum with advanced fibrosis, indicating s significant difference in serum miR-29a levels in the advanced stage of liver fibrosis. Understanding of the behavior changes of serum miR-29 during the progression of NASH/NAFLD-induced liver fibrosis remained limited although miR-29 has been linked to various types of fibrosis. Therefore, further study of serum miR-29 is warranted in the future.

Table I. Histological examination of the NAFLD/NASH liver in mice.

| Histopathological changes | 1 week | 2 weeks | 6 weeks |
|---|---|---|---|
| Steatosis | Grade2 | Grade3 | Grade3 |
| Inflammation | Grade1 | Grade2 | Grade3 |
| Ballooning | Grade0 | Grade2 | Grade3 |
| Fibrosis | Grade0 | Grade0 | Grade2 |

Some of the miRNAs in Tables II and III identified in this study include those previously reported by other researchers. The miRNA expression changes observed in this study are likely to be closely associated with liver fibrosis. However, many other miRNAs are also altered in expression at the same time, suggesting that fibrosis is regulated by a complex network of miRNAs and cytokines other than miR-29, which are also associated with fibrosis. For example, TGF-β/Smad has been detected in Table SI as a signal related to fibrosis other than collagen, and miR-122-5p is predicted to be a miRNA associated with this pathway. miR-122-5p has been reported to be associated with the TGF-β signaling pathway in liver fibrosis (36,37). On the other hand, TNF-α is known to be another molecule involved in liver fibrosis besides miRNAs, which induces liver fibrosis by causing activation of hepatic astrocytes (38). Therefore, a comprehensive interpretation including molecules other than miRNAs will be required to fully understand the mechanism of fibrosis development.

The clinical significance of this study is that it may be possible to detect fibrosis in patients with suspected NASH without a liver biopsy, and that measurement of miR-29 may aid in the diagnosis of early fibrosis. While the treatment of NASH generally involves improvement of the underlying disease, exercise, and diet, this study suggests a role for miR-29 in inhibiting fibrosis, which may allow miR-29 to be used as a treatment for NASH. Replenishing the liver with miR-29 as a new treatment may improve or inhibit the progression of liver fibrosis.

In this study we identified miR-29 as an early marker of NASH liver fibrosis in mice. Although miRNAs are highly conserved between humans and mice, the dynamics of miRNAs in blood may differ in human NASH versus mice. A previous study found that miR-29 levels are elevated in NAFLD/NASH serum in humans (34), but the blood dynamics of miR-29 in patients with NASH have been reported only in

Table II. Differences in the expression levels of miRNAs in the liver of NASH model mice fed for 2 weeks.

| miRNA name | Accession no. | Fold-change | Up/down |
|---|---|---|---|
| miR-1224-5p | MIMAT0005460 | 1.75 | Up |
| miR-15b-5p | MIMAT0000124 | 1.50 | Up |
| miR-223-3p | MIMAT0000665 | 2.43 | Up |
| miR-342-3p | MIMAT0000590 | 4.44 | Up |
| miR-34a-5p | MIMAT0000542 | 6.03 | Up |
| miR-3960 | MIMAT0019336 | 3.86 | Up |
| miR-5126 | MIMAT0020637 | 2.90 | Up |
| miR-7118-5p | MIMAT0028133 | 9.94 | Up |
| miR-8110 | MIMAT0031416 | 4.91 | Up |
| let-7a-5p | MIMAT0000521 | -1.61 | Down |
| let-7b-5p | MIMAT0000522 | -1.54 | Down |
| let-7c-5p | MIMAT0000523 | -1.54 | Down |
| let-7f-5p | MIMAT0000525 | -2.52 | Down |
| let-7g-5p | MIMAT0000121 | -2.85 | Down |
| miR-101a-3p | MIMAT0000133 | -4.63 | Down |
| miR-101c | MIMAT0019349 | -5.55 | Down |
| miR-103-3p | MIMAT0000546 | -1.62 | Down |
| miR-107-3p | MIMAT0000647 | -1.82 | Down |
| miR-10a-5p | MIMAT0000648 | -1.84 | Down |
| miR-122-3p | MIMAT0017005 | -5.11 | Down |
| miR-122-5p | MIMAT0000246 | -2.87 | Down |
| miR-126a-3p | MIMAT0000138 | -2.19 | Down |
| miR-130a-3p | MIMAT0000141 | -1.59 | Down |
| miR-148a-3p | MIMAT0000516 | -2.37 | Down |
| miR-15a-5p | MIMAT0000526 | -2.50 | Down |
| miR-16-5p | MIMAT0000527 | -1.71 | Down |
| miR-192-5p | MIMAT0000517 | -3.87 | Down |
| miR-193a-3p | MIMAT0000223 | -2.60 | Down |
| miR-194-5p | MIMAT0000224 | -3.07 | Down |
| miR-19a-3p | MIMAT0000651 | -3.79 | Down |
| miR-19b-3p | MIMAT0000513 | -3.87 | Down |
| miR-20a-5p | MIMAT0000529 | -2.02 | Down |
| miR-20b-5p | MIMAT0003187 | -1.93 | Down |
| miR-21a-5p | MIMAT0000530 | -1.82 | Down |
| miR-22-3p | MIMAT0000531 | -2.34 | Down |
| miR-23b-3p | MIMAT0000125 | -1.92 | Down |
| miR-26a-5p | MIMAT0000533 | -2.09 | Down |
| miR-26b-5p | MIMAT0000534 | -3.25 | Down |
| miR-27b-3p | MIMAT0000126 | -1.93 | Down |
| miR-29a-3p | MIMAT0000535 | -1.74 | Down |
| miR-29b-3p | MIMAT0000127 | -2.28 | Down |
| miR-29c-3p | MIMAT0000536 | -2.59 | Down |
| miR-30a-3p | MIMAT0000129 | -2.37 | Down |
| miR-30a-5p | MIMAT0000128 | -2.40 | Down |
| miR-30b-5p | MIMAT0000130 | -2.83 | Down |
| miR-30c-5p | MIMAT0000514 | -2.51 | Down |
| miR-30d-5p | MIMAT0000515 | -1.68 | Down |
| miR-30e-5p | MIMAT0000248 | -2.93 | Down |
| miR-365-3p | MIMAT0000711 | -2.35 | Down |
| miR-3963 | MIMAT0019341 | -2.83 | Down |
| miR-3968 | MIMAT0019352 | -3.15 | Down |

Table II. Continued.

| miRNA name | Accession no. | Fold-change | Up/down |
|---|---|---|---|
| miR-451a | MIMAT0001632 | -3.66 | Down |
| miR-5100 | MIMAT0020607 | -3.12 | Down |
| miR-6366 | MIMAT0025110 | -1.66 | Down |
| miR-6368 | MIMAT0025112 | -1.52 | Down |
| miR-99a-5p | MIMAT0000131 | -1.62 | Down |

miR, microRNA.

Table III. Differences in the expression levels of miRNAs in the serum of NASH model mice fed for 2 weeks.

| miRNA name | Accession no. | Fold-change | Up/down |
|---|---|---|---|
| let-7c-5p | MIMAT0000523 | 1.59 | Up |
| let-7i-5p | MIMAT0000122 | 1.59 | Up |
| miR-122-5p | MIMAT0000246 | 26.58 | Up |
| miR-130a-3p | MIMAT0000141 | 1.73 | Up |
| miR-148a-3p | MIMAT0000516 | 5.00 | Up |
| miR-16-5p | MIMAT0000527 | 1.75 | Up |
| miR-192-5p | MIMAT0000517 | 8.60 | Up |
| miR-21a-5p | MIMAT0000530 | 2.85 | Up |
| miR-22-3p | MIMAT0000531 | 2.11 | Up |
| miR-27a-3p | MIMAT0000537 | 1.56 | Up |
| miR-2861 | MIMAT0013803 | 1.79 | Up |
| miR-29a-3p | MIMAT0000535 | 1.55 | Up |
| miR-29c-3p | MIMAT0000536 | 2.22 | Up |
| miR-30a-5p | MIMAT0000128 | 1.79 | Up |
| miR-342-3p | MIMAT0000590 | 3.03 | Up |
| miR-3473f | MIMAT0031390 | 1.53 | Up |
| miR-34a-5p | MIMAT0000542 | 5.28 | Up |
| miR-3960 | MIMAT0019336 | 2.36 | Up |
| miR-6931-5p | MIMAT0027762 | 2.79 | Up |
| miR-7118-5p | MIMAT0028133 | 1.54 | Up |
| miR-8110 | MIMAT0031416 | 1.58 | Up |
| miR-133a-3p | MIMAT0000145 | -3.03 | Down |
| miR-133b-3p | MIMAT0000769 | -2.97 | Down |
| miR-140-3p | MIMAT0000152 | -1.97 | Down |
| miR-1897-5p | MIMAT0007864 | -1.69 | Down |
| miR-486a-5p | MIMAT0003130 | -2.54 | Down |
| miR-6366 | MIMAT0025110 | -1.86 | Down |
| miR-7047-5p | MIMAT0027998 | -2.84 | Down |

miR, microRNA.

a few cases and will need to be investigated in more detail in the future.

In humans, however, NAFLD/NASH is frequently linked to underlying conditions such as obesity, hypertension, dyslipidemia, and diabetes (39,40). This study used mice without underlying diseases such as diabetes. In this study, miR-29

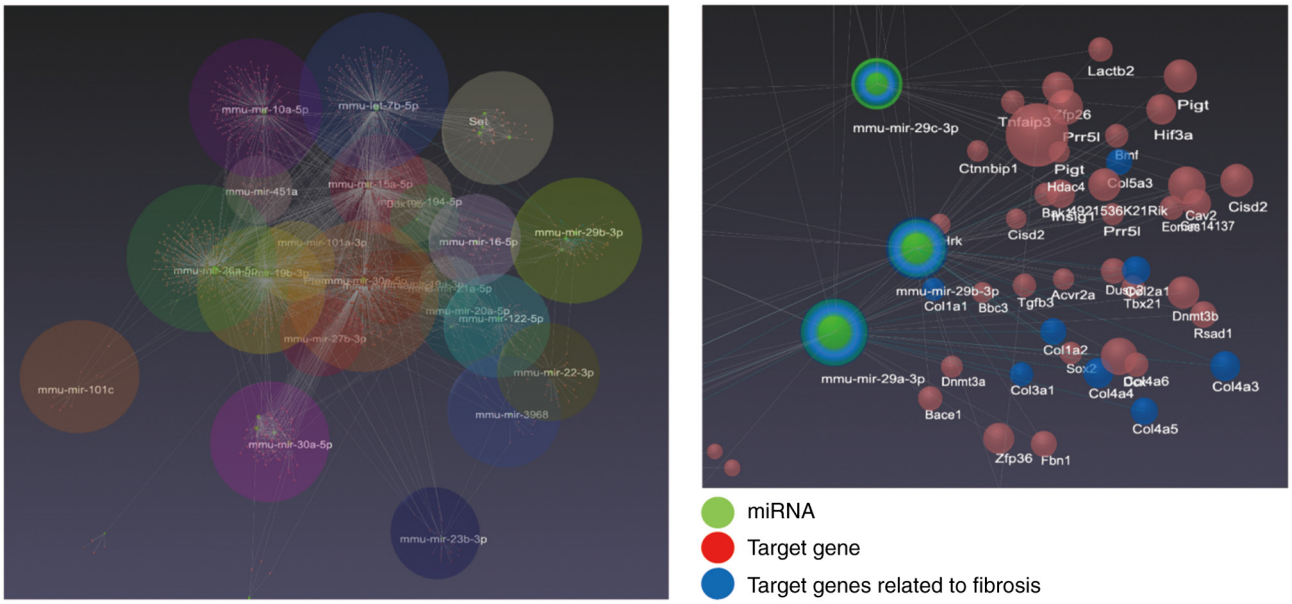


Figure 3. Prediction and biological interpretation of miRNA target genes using OmicsNet. OmicsNet was used to predict target genes and functions associated with liver fibrosis for 47 downregulated miRNAs identified thought miRNA microarray analysis of control and NASH liver 2 weeks after high-fat diet feeding. The present study used 'collagen biogenesis and modifying enzyme' and 'collagen formation' in the Reactome database of OmicsNet to predict fibrosis-related target genes. Lines connect miRNA target genes to their related functions. The enlarged figure shows green circles for miRNAs, red circles for target genes and blue circles for fibrosis-related target genes. miRNA; microRNA.

was increased in the blood when mice without underlying disease were used in the early stages of fibrosis. However, the blood miR-29 kinetics in mice with underlying disease are not clear. Also, the relationship between the underlying disease and miR-29 is not clear at this time. The type of fat in the diet used for feeding may also affect the experimental results. Therefore, it is necessary to analyze the changes in miR-29 expression in mouse models with underlying diseases, such as diabetes, in the future.

Also, although we used CDAHDF to rapidly induce NASH in this study, there are several known diets of laboratory animals that induce NASH, each with different fat components and other nutrients in the diet. It is possible that the type of fat that accumulates in the liver may differ depending on the diet used. Therefore, it is necessary to understand the differences in the types of fat that accumulate in the liver with different NASH-inducing diets used and to verify in the future which diets are more similar to the fat components of the human NASH condition.

## Acknowledgements

Not applicable.

## Funding

The present study was supported in part by The JSPS KAKENHI (grant nos. 21H04844 and 20K21692).

## Availability of data and materials

The datasets used and/or analyzed during the current study are available from the corresponding author on reasonable request. The datasets generated and/or analyzed during the current study are available in the Gene Expression Omnibus repository (https://www.ncbi.nlm.nih.gov/geo/query/acc.cgi?acc=GSE252035).

## Authors' contributions

KM and MC were major contributors in performing the experiments and writing the manuscript. YO, CT, MH, YK, and MO helped conduct the experiments. All authors read and approved the final manuscript. KM and MC confirm the authenticity of all the raw data.

## Ethics approval and consent to participate

All experiments were performed following The Guideline for Animal Experimentation of Hirosaki University. The Animal Research Committee of Hirosaki University (approval no. AE01-2023-004) approved and monitored the procedures.

## Patient consent for publication

Not applicable.

## Competing interests

The authors declare that they have no competing interests.

## References

1. Hashimoto E, Taniai M and Tokushige K: Characteristics and diagnosis of NAFLD/NASH. J Gastroenterol Hepatol 28: 64-70, 2013.
2. Younossi ZM, Golabi P, Paik JM, Henry A, Van Dongen C and Henry L: The global epidemiology of nonalcoholic fatty liver disease (NAFLD) and nonalcoholic steatohepatitis (NASH): A systematic review. Hepatology 77: 1335-1347, 2023

3. Parthasarathy G, Revelo X and Malhi H: Pathogenesis of nonalcoholic steatohepatitis: An overview. Hepatol Commun 4: 478-492, 2020.
4. Fraile JM, Palliyil S, Barelle C, Porter AJ and Kovaleva M: Non-alcoholic steatohepatitis (NASH)-A review of a crowded clinical landscape, driven by a complex disease. Drug Des Dev Ther 15: 3997-4009, 2021.
5. Sanyal AJ, Van Natta ML, Clark J, Neuschwander-Tetri BA, Diehl A, Dasarathy S, Loomba R, Chalasani N, Kowdley K, Hameed B, *et al*: Prospective study of outcomes in adults with nonalcoholic fatty liver disease. N Engl J Med 385: 1559-1569, 2021.
6. Schuppan D, Surabattula R and Wang XY: Determinants of fibrosis progression and regression in NASH. J Hepatol 68: 238-250, 2018.
7. European Association for the Study of the Liver. Electronic address: easloffice@easloffice.eu; Clinical Practice Guideline Panel, Chair:; EASL Governing Board representative:; and Panel members: EASL clinical practice guidelines on non-invasive tests for evaluation of liver disease severity and prognosis-2021 update. J Hepatol 75: 659-689, 2021.
8. Ratziu V, Charlotte F, Heurtier A, Gombert S, Giral P, Bruckert E, Grimaldi A, Capron F and Poynard T; LIDO study group: Sampling variability of liver biopsy in nonalcoholic fatty liver disease. Gastroenterology 128: 1898-1906, 2005.
9. Merriman RB, Ferrell LD, Patti MG, Weston SR, Pabst MS, Aouizerat BE and Bass NM: Correlation of paired liver biopsies in morbidly obese patients with suspected nonalcoholic fatty liver disease. Hepatology 44: 874-880, 2006.
10. Ajmera V and Loomba R: Imaging biomarkers of NAFLD, NASH, and fibrosis. Mol Metab 50: 101167, 2021.
11. Seko Y, Sumida Y, Tanaka S, Mori K, Taketani H, Ishiba H, Hara T, Okajima A, Yamaguchi K, Moriguchi M, *et al*: Serum alanine aminotransferase predicts the histological course of non-alcoholic steatohepatitis in Japanese patients. Hepatol Res 45: E53-E61, 2015.
12. McGill MR: The past and present of serum aminotransferases and the future of liver injury biomarkers. Excli J 15: 817-828, 2016.
13. Kruger FC, Daniels CR, Kidd M, Swart G, Brundyn K, van Rensburg C and Kotze M: APRI: A simple bedside marker for advanced fibrosis that can avoid liver biopsy in patients with NAFLD/NASH. S Afr Med J 101: 477-480, 2011.
14. Shah AG, Lydecker A, Murray K, Tetri BN, Contos MJ and Sanyal AJ; Nash Clinical Research Network: Comparison of noninvasive markers of fibrosis in patients with nonalcoholic fatty liver disease. Clin Gastroenterol Hepatol 7: 1104-1112, 2009.
15. Angulo P, Hui JM, Marchesini G, Bugianesi E, George J, Farrell GC, Enders F, Saksena S, Burt AD, Bida JP, *et al*: The NAFLD fibrosis score: A noninvasive system that identifies liver fibrosis in patients with NAFLD. Hepatology 45: 846-854, 2007.
16. Wieckowska A, Zein NN, Yerian LM, Lopez AR, McCullough AJ and Feldstein AE: In vivo assessment of liver cell apoptosis as a novel biomarker of disease severity in nonalcoholic fatty liver disease. Hepatology 44: 27-33, 2006.
17. Pimentel CF, Jiang ZG, Otsubo T, Feldbrügge L, Challies TL, Nasser I, Robson S, Afdhal N and Lai M: Poor inter-test reliability between CK18 kits as a biomarker of NASH. Dig Dis Sci 61: 905-912, 2016.
18. Cusi K, Chang Z, Harrison S, Lomonaco R, Bril F, Orsak B, Ortiz-Lopez C, Hecht J, Feldstein AE, Webb A, *et al*: Limited value of plasma cytokeratin-18 as a biomarker for NASH and fibrosis in patients with non-alcoholic fatty liver disease. J Hepatol 60: 167-174, 2014.
19. Felekkis K, Touvana E, Stefanou Ch and Deltas C: MicroRNAs: A newly described class of encoded molecules that play a role in health and disease. Hippokratia 14: 236-240, 2010.
20. Saliminejad K, Khorshid HR, Fard SS and Ghaffari SH: An overview of microRNAs: Biology, functions, therapeutics, and analysis methods. J Cell Physiol 234: 5451-5465, 2019.
21. Yu X, Odenthal M and Fries JW: Exosomes as miRNA carriers: Formation-function-future. Int J Mol Sci 17: 2028, 2016.
22. Kleiner DE, Brunt EM, Van Natta M, Behling C, Contos MJ, Cummings OW, Ferrell LD, Liu YC, Torbenson MS, Unalp-Arida A, *et al*: Design and validation of a histological scoring system for nonalcoholic fatty liver disease. Hepatology 41: 1313-1321, 2005.
23. Matsumoto M, Hada N, Sakamaki Y, Uno A, Shiga T, Tanaka C, Ito T, Katsume A and Sudoh M: An improved mouse model that rapidly develops fibrosis in non-alcoholic steatohepatitis. Int J Exp Pathol 94: 93-103, 2013.
24. Wang M, Huo Z, He X, Liu F, Liang J, Wu L and Yang D: The role of MiR-29 in the mechanism of fibrosis. Mini Rev Med Chem 23: 1846-1858, 2023.
25. Ebada MA, Mostafa A, Gadallah AHA, Alkanj S, Alghamdi BS, Ashraf GM, Abuzenadah AM, Alserihi RF, Wadaa-Allah A and Salama M: Potential regulation of miRNA-29 and miRNA-9 by estrogens in neurodegenerative disorders: An insightful perspective. Brain Sci 13: 243, 2023.
26. Amirian M, Jafari-Nozad AM, Darroudi M, Farkhondeh T and Samarghandian S: Overview of the miR-29 family members' function in breast cancer. Int J Biol Macromol 230: 123280, 2023.
27. Wang T, Li Y, Chen J, Xie L and Xiao T: TGF-β1/Smad3 signaling promotes collagen synthesis in pulmonary artery smooth muscle by down-regulating miR-29b. Int J Clin Exp Pathol 11: 5592-5601, 2018.
28. Ezhilarasan D: MicroRNA interplay between hepatic stellate cell quiescence and activation. Eur J Pharmacol 885: 173507, 2020.
29. Matsumoto Y, Itami S, Kuroda M, Yoshizato K, Kawada N and Murakami Y: MiR-29a assists in preventing the activation of human stellate cells and promotes recovery from liver fibrosis in mice. Mol Ther 24: 1848-1859, 2016.
30. Lin HY, Wang FS, Yang YL and Huang YH: MicroRNA-29a suppresses CD36 to ameliorate high fat diet-induced steatohepatitis and liver fibrosis in mice. Cells 8: 1298, 2019.
31. López-Riera M, Conde I, Quintas G, Pedrola L, Zaragoza Á, Perez-Rojas J, Salcedo M, Benlloch S, Castell JV and Jover R: Non-invasive prediction of NAFLD severity: A comprehensive, independent validation of previously postulated serum microRNA biomarkers. Sci Rep 8: 10606, 2018.
32. Kim TH, Lee Y, Lee YS, Gim JA, Ko E, Yim SY, Jung YK, Kang S, Kim MY, Kim H, *et al*: Circulating miRNA is a useful diagnostic biomarker for nonalcoholic steatohepatitis in nonalcoholic fatty liver disease. Sci Rep 11: 14639, 2021.
33. Liu J, Xiao Y, Wu X, Jiang L, Yang S, Ding Z, Fang Z, Hua H, Kirby MS and Shou J: A circulating microRNA signature as noninvasive diagnostic and prognostic biomarkers for nonalcoholic steatohepatitis. BMC Genomics 19: 188, 2018.
34. Khalifa O, Errafii K, Al-Akl NS and Arredouani A: Noncoding RNAs in nonalcoholic fatty liver disease: Potential diagnosis and prognosis biomarkers. Dis Markers 2020: 8822859, 2020.
35. Jampoka K, Muangpaisarn P, Khongnomnan K, Treeprasertsuk S, Tangkijvanich P and Payungporn S: Serum miR-29a and miR-122 as potential biomarkers for non-alcoholic fatty liver disease (NAFLD). Microrna 7: 215-222, 2018.
36. Zhou Z, Zhang R, Li X, Zhang W, Zhan Y, Lang Z, Tao Q, Yu J, Yu S, Yu Z and Zheng J: Circular RNA cVIM promotes hepatic stellate cell activation in liver fibrosis via miR-122-5p/miR-9-5p-mediated TGF-β signaling cascade. Commun Biol 7: 113, 2024.
37. Sun Y, Wang H, Li Y, Liu S, Chen J and Ying H: MiR-24 and miR-122 negatively regulate the transforming growth factor-β/Smad signaling pathway in skeletal muscle fibrosis. Mol Ther Nucleic Acids 11: 528-537, 2018.
38. Xu R, Zhang Z and Wang FS: Liver fibrosis: Mechanisms of immune-mediated liver injury. Cell Mol Immunol 9: 296-301, 2012.
39. Dietrich P and Hellerbrand C: Non-alcoholic fatty liver disease, obesity and the metabolic syndrome. Best Pract Res Clin Gastroenterol 28: 637-653, 2014.
40. Younossi ZM, Koenig AB, Abdelatif D, Fazel Y, Henry L and Wymer M: Global epidemiology of nonalcoholic fatty liver disease-meta-analytic assessment of prevalence, incidence, and outcomes. Hepatology 64: 73-84, 2016.